Heat-Transfer and Ablation-Rate Correlations for Re-Entry Heat-Shield and Nosetip Applications

KURT E. PUTZ*
Sandia Laboratories, Albuquerque, N.Mex.
AND
EUGENE P. BARTLETT†
Aerotherm Division of Acurex Corporation, Mountain View, Calif.

Blowing-correction correlation equations for heat- and mass-transfer coefficients are presented and compared with theoretical boundary-layer solutions and some recent R/V flight thermal data. The correlations are based on stagnation-point chemically-reacting (equilibrium) boundary-layer solutions considering graphite, carbon phenolic, or nylon phenolic ablation under typical ballistic entry conditions (H_e ranging from 500 to 13,000 Btu/lb and P_{T_2} from 0.01 to 150 atm). The matrix of solutions and resulting correlation equations are sufficiently general that they are expected to apply to other ablation materials and flight conditions as well as long as the principal surface material is graphitic or carbonaceous char. The correlations are also applied to and compared with solutions for the nonsimilar laminar or turbulent boundary layer around sphere cone bodies. A procedure is also demonstrated for predicting heat-shield response where transfer coefficients are given directly by boundary-layer solutions. Resulting predictions for heat-transfer, ablation rates, and in-depth temperatures obtained with the two approaches are seen to agree well with each other and flight thermal data.

Nomenclature

B' = blowing parameter, $\dot{m}_w/\rho_e u_e C_M$
B_o' = blowing parameter, $\dot{m}_w/\rho_e u_e C_{H_o}'$
C_H, C_H' = heat-transfer coefficients defined implicity by Eq. (5) and Eq. (7)
C_{H_o}' = nonablating heat-transfer coefficient defined implicitly by Eq. (8)
C_M = mass-transfer coefficient defined implicitly by Eq. (3)
C_{M_i}, C_{M_k} = mass-transfer coefficient for species i, element k
h, h_i = static enthalpy, enthalpy of species i, Btu/lb
H_r, H = recovery enthalpy, total enthalpy, Btu/lb
$\tilde{j}_{k_w}$ = diffusional mass flux of element k at wall, lb/sec-ft^2
K_i = mass fraction of species i
$\tilde{K}_k$ = mass fraction of element k irrespective of molecular configuration [Eq. (2)]
Le_f = Lewis number based on frozen Prandtl number
$\dot{m}$ = mass-flow rate per unit area, lb/sec-ft^2
$\dot{m}_w$ = net mass flux of vapor into the boundary layer $\dot{m}_g + \dot{m}_c$) in the absence of mechanical ablation, lb/sec-ft^2
$\mathcal{M}$ = molecular weight, lb/lb-mole
n = exponent in Lewis number correlation [Eq. (6)]
P_{T_2} = total pressure behind bow shock, atm
q_{ref} = reference heat flux defined by Eq. (10), Btu/sec-ft^2
q_w = net surface heat flux, Btu/sec-ft^2
R_N = nose radius, in.
s = streamwise coordinate, in.
T = temperature, °R
u_e = velocity at edge of boundary layer, ft/sec
α_{ki} = mass fraction of element k in species i
ΔH_c = heat-transfer correlation parameter defined implicitly by Eq. (9) and given by Eq. (14), Btu/lb
θ_c = cone half-angle, degrees
λ_m = mass-transfer correlation parameter defined implicitly by Eq. (11) and given by Eq. (12)
ρ = density, lb/ft^3
ψ = heat-transfer correlation parameter defined implicitly by Eq. (9) and given by Eq. (13)

Subscripts

c = char or solid material; also pertaining to correlation
e = evaluated at edge of boundary layer
fe = evaluated at frozen edge state
g = resin off-gas
i = gaseous species
k = element
o = nonablating
ss = steady state
w = evaluated at wall

Introduction

THE transient response of a homogeneous or charring ablator is dependent on the chemically reacting boundary-layer flow adjacent to the surface, and vice versa. This mutual dependence results in direct coupling between the ablation material response and the adjacent chemically reacting flow. Solution of this coupled problem has typically taken two avenues of approach, intimate coupling and transfer coefficient. Intimate coupling of a transient indepth heat-conduction procedure to a chemically reacting boundary-layer procedure was accomplished in Ref. 1. While this procedure yields excellent solutions, in general the computer time required to obtain a solution for routine design problems is prohibitive.

The film or transfer-coefficient approach attempts to simplify the problem by separating the transient in-depth heat-conduction procedure from a chemically-reacting boundary-layer procedure. In this method, heat- and mass-transfer coefficients are employed to represent the convective heat- and mass-transfer rates at the ablating material surface. Various degrees of coupling can be accomplished by satisfying conservation of mass and energy at the ablating surface. Potentially this approach can yield the intimately coupled solution as obtained above if the transfer coefficients are based on chemically-reacting boundary-layer solutions.

Heat- and mass-transfer coefficient approaches have proven to be very useful for correlating theoretical as well as experimental heat- and mass-transfer results for nonreacting boundary-layer flows. They also have been used with success to correlate

Presented as Paper 72-91 at the AIAA 10th Aerospace Sciences Meeting, San Diego, Calif., January 17–19, 1972; submitted March 10, 1972; revision received September 14, 1972. This work was supported by the U.S. Atomic Energy Commission.

Index categories: Material Ablation; Boundary Layers and Convective Heat Transfer—Laminar; Boundary Layers and Convective Heat Transfer—Turbulent.

* Technical Staff Member, R/V Aerothermodynamics Division. Member AIAA.

† Manager of Aerosciences Department. Member AIAA.

the results of chemically-reacting boundary-layer calculations. Techniques which have worked well for these simplified flows have been applied extensively to flow situations involving chemically-reacting boundary layers over ablating bodies. With the advent of a solution procedure for the chemically-reacting boundary layer coupled with surface ablation response,[2] it is now possible to investigate the errors associated with applying non-reacting boundary-layer correlation procedures to reacting flows and to suggest improved correlation approaches.

Stagnation-point heat- and mass-transfer coefficient correlations are developed which are applicable over a broad range of re-entry conditions to carbons and reinforced plastics which form carbonaceous chars. These correlations are then applied to positions around the body and compared to nonsimilar laminar and turbulent boundary-layer solution data. A procedure is also demonstrated for predicting heat-shield ablation and thermal response where transfer coefficients are given directly by chemically-reacting boundary-layer solutions without intermediary correlations. Agreement between the transfer-coefficient correlations, the direct approach, and heat-shield flight data is seen to be excellent.

Boundary-Layer Solution Procedure

The basic boundary-layer solution data from which the transfer coefficients were calculated were generated with the BLIMP computer code.[3] BLIMP is based on an analysis and computational approach described in Refs. 2 and 4. It solves for the chemically-reacting laminar or turbulent boundary layer around axisymmetric or planar bodies. It considers equilibrium chemistry throughout the boundary layer for a general chemical system. It admits mass addition at the surface while considering surface equilibrium (when desired) and a surface energy balance (when desired). Other options permit the specification of surface ablation rates, pyrolysis gas rates, and/or surface temperatures. At the boundary-layer edge, entropy layer effects can be considered through specification of the shock shape. Otherwise, the boundary-layer edge expansion is assumed to be isentropic.

While a similarity transformation is employed for convenience, all nonsimilar terms are retained. Laminar boundary-layer solutions are thus accurate within the constraints of equilibrium, the accuracy of the thermodynamic (JANAF) and transport properties of the individual species and of the mixture, and the validity of the boundary-layer equations. Diffusion coefficients are considered equal in the present study, but the code has the capability of considering unequal diffusion effects.

The particular approach employed to represent equal diffusion coefficients in BLIMP is rather unique and therefore needs some explanation. It is based on an "effective" diffusion coefficient $\mathscr{D}_{\text{eff}}$ which is like a self-diffusion coefficient for a "species" representative of the local mixture.[5] Thus, in the case of massive hydrogen injection into a nitrogen boundary layer, the $\mathscr{D}_{\text{eff}}$ varies across the boundary layer from a value near the wall which approaches the self-diffusion coefficient of hydrogen to a value at the edge equivalent to the self-diffusion coefficient of nitrogen. This is to be contrasted to the more typical approach where a binary diffusion coefficient based on injectant and edge gas "species" is employed throughout the boundary layer.

Transfer-Coefficient Approaches

The film- or transfer-coefficient approach for representing boundary-layer heat- and mass-transfer characteristics has been used extensively in the re-entry aerothermodynamics community. Basically, the approach is to relate wall fluxes to driving potentials by means of transfer coefficients. Given specific definitions of the driving potentials, the problem of representing surface heat and mass fluxes reduces to that of evaluating the transfer coefficients for a given situation. The usual approach has been to start with a nonablating heat-transfer coefficient obtained by whatever means available, to correct this coefficient for mass addition by use of a blowing correction obtained from simple (e.g., inert injection) boundary-layer solutions or from a correlation of experimental data, and to calculate a mass-transfer coefficient through use of the Chilton-Colburn analogy which relates heat- and mass-transfer coefficients. Several alternative mass- and heat-transfer coefficient approaches are described in the following subsections.

Mass-Transfer Coefficient

For an equilibrium boundary layer with assumed equal diffusion coefficients it is convenient to relate the diffusional mass flux of element k at the wall $\tilde{j}_{k_w}$ to a $\tilde{K}_k$ driving potential by defining an elemental mass-transfer coefficient $\rho_e u_e C_{M_k}$[5]

$$\tilde{j}_{k_w} = -\rho_e u_e C_{M_k}(\tilde{K}_{k_e} - \tilde{K}_{k_w}) \tag{1}$$

where $\tilde{K}_k$ is the mass fraction of element k irrespective of molecular configuration.

$$\tilde{K}_k = \sum_i \alpha_{ki} K_i \tag{2}$$

In the case of a similar boundary layer and in fact for many nonsimilar boundary-layer problems of interest, the $\rho_e u_e C_{M_k}$ are identical for all elements k and Eq. (1) can be simplified to

$$\tilde{j}_{k_w} = \rho_e u_e C_M(\tilde{K}_{k_e} - \tilde{K}_{k_w}) \tag{3}$$

For nonsimilar boundary-layer problems, the $\rho_e u_e C_{M_k}$ will differ in general even for assumed equal diffusion coefficients if there are more than two effective components, namely, if the elemental composition of the edge gas or injected material varies with streamwise position. Ablation of a noncharring material such as graphite in equilibrium air is a two-component problem as is the steady-state ablation of a charring material for which the ratio of $\dot{m}_g$ to $\dot{m}_c$ is a constant dependent only on the virgin material composition.

Since it is only recently that nonsimilar boundary-layer codes with ablating wall boundary conditions have become available to provide nonsimilar $\rho_e u_e C_{M_k}$ data, it has been common practice to employ a single $\rho_e u_e C_M$ in ablation studies.[6] Now that nonsimilar mass-transfer solutions can be generated with the BLIMP code,[3] one could attempt to correlate individual $\rho_e u_e C_{M_k}$ data. However, this was not done in the present study.

Heat-Transfer Coefficient

The energy flux to a nonablating wall consists of molecular conduction and diffusion. It is convenient to divide this flux into terms representing the convection of sensible enthalpy measured above some base temperature and the diffusion of chemical energy at this base temperature. The first term is characterized by a heat-transfer coefficient and a sensible enthalpy driving potential, whereas the second is represented by a mass-transfer coefficient, concentration driving potentials, and chemical enthalpy terms.

In the case of frozen boundary layers with catalytic walls, it is appropriate to select the wall temperature as the base temperature. It has been shown by several investigators[7-9] that the correlation equation logically takes the form

$$q_w = \rho_e u_e C_H \left[(H_r - h_w)_{fe} + \sum_i (C_{M_i}/C_H)(K_{i_e} - K_{i_w}) h_{i_w} \right] \tag{4}$$

where $\rho_e u_e C_{M_i}$ is the mass-transfer coefficient for species i, h_i is the enthalpy of species i, and the subscript fe is used to signify that $(H_r - h_w)$ is evaluated at the frozen edge state. If attention is limited to equal-diffusion similar boundary layers or nonsimilar boundary layers with two effective components, the $\rho_e u_e C_{M_i}$ are all equal and Eq. (4) can be simplified to

$$q_w = \rho_e u_e C_H \left[(H_r - h_w)_{fe} + (C_M/C_H) \sum_i (K_{i_e} - K_{i_w}) h_{i_w} \right] \tag{5}$$

The Chilton-Colburn relation is typically used to relate C_M/C_H to a frozen Lewis number. For example, Ref. 6 suggests

$$C_M/C_H = Le_f^n \tag{6}$$

with $n = \frac{2}{3}$ recommended for general use.‡

Rosner[8] employs the concept of "equilibrium thermal conductivity" to obtain a plausible expression for stagnation-point boundary layers in local thermochemical equilibrium. He concludes that if atom recombination takes place the resulting heat transfer is often about the same regardless of whether the recombination occurs solely as a result of surface reaction or at equilibrium within the gas phase. This result is consistent with the classic results of Fay and Riddell[10] who correlated a number of stagnation-point air boundary-layer solutions.

Encouraged by this result, Rosner suggests the tentative use of Eq. (4) for representing energy transport in a multicomponent, chemically-reacting system. He points out that this approach should be valid for Lewis and Prandtl numbers near unity but that when these parameters differ substantially from unity, success depends upon the degree of coupling between the equations of motion, species conservation, and energy equations.

Spalding[9] is less encouraging with regard to applying Eq. (4) to reacting systems. To the contrary, he suggests that it might be more accurate to express the wall heat flux in terms of a total enthalpy driving potential. He points out that Eq. (4) would be particularly suspect if energetic reactions occur well into the boundary layer away from the surface.

Spalding also cautions against the use of Eq. (6) when there is net mass transfer at the surface. He presents the results of laminar flat-plate nonreacting boundary-layer solutions with blowing and suction which demonstrate that the Lewis number exponent n deviates from $\frac{2}{3}$ for large net mass transfer. This is consistent with Lees[11] who crossplotted the results of Mickley et al.[12] and found $n \approx \frac{2}{3}$ for zero mass transfer, $n \approx 1$ for moderate mass transfer, and $n \approx 2$ for large mass transfer (near boundary-layer blowoff) for these data. It would appear from this that mass addition may not negate the use of the Chilton-Colburn relation considered above, but may necessitate the development of a Lewis number correlation equation which is more complicated than Eq. (6) with n taken to be $\frac{2}{3}$.

Following the suggestion of Spalding it may be useful, for injection into a chemically active boundary layer, to express the wall heat flux in terms of a simple equilibrium enthalpy potential

$$q_w = \rho_e u_e C_H'(H_e - h_w) \tag{7}$$

where H_e is the total enthalpy of the edge gas, h_w is the enthalpy of the gas mixture at the wall, and the prime has been introduced to distinguish $\rho_e u_e C_H'$ from the $\rho_e u_e C_H$ of Eq. (5). Alternatively, for positions away from the stagnation point, one might want to consider replacing H_e in Eq. (7) by the recovery enthalpy H_r. When this is done it might be noted from Eq. (5) that $\rho_e u_e C_H'$ and $\rho_e u_e C_H$ are identical for the special case when C_M/C_H is unity.

In developing heat- and mass-transfer coefficient correlations, it is often convenient to consider a nonablating transfer coefficient multiplied by a blowing correction. The most straightforward approach would appear to be to normalize $\rho_e u_e C_M$, $\rho_e u_e C_H$, and $\rho_e u_e C_H'$ by $\rho_e u_e C_{M_o}$, $\rho_e u_e C_{H_o}$, and $\rho_e u_e C_{H_o}'$, respectively, where the $\rho_e u_e C_{M_o}$, etc., would be obtained as the limiting case of $\rho_e u_e C_M$, etc., as the surface mass-transfer rate is reduced to zero. This is possible for $\rho_e u_e C_{H_o}'$ since one can define§

$$q_{w_o} = \rho_e u_e C_{H_o}'(H_e - h_w) \tag{8}$$

and $\rho_e u_e C_{H_o}'$ can be calculated from an air boundary-layer solution at the ablation temperature. Conversely, $\rho_e u_e C_{M_o}$ (and hence also $\rho_e u_e C_{H_o}$) is not simply defined for zero mass transfer. Therefore, it is convenient to employ $\rho_e u_e C_{H_o}'$ as the normalizing parameter for $\rho_e u_e C_M$ and $\rho_e u_e C_H$ as well as $\rho_e u_e C_H'$.

For some applications, it is useful to correlate heat-transfer rates directly. For example, in the present studies, q_w is expressed as

$$q_w/q_{\text{ref}} = [\psi(H_e - h_w)/H_e] + [\Delta H_c/H_e] \tag{9}$$

where ψ is like a blowing reduction parameter [identically equal to C_H'/C_{H_o}' when $\Delta H_c = 0$, see Eq. (7) and Eq. (10)], ΔH_c is a second correlation parameter to account for gas-phase reactions and/or nonunity Lewis number effects involving injected species, and q_{ref} is defined by

$$q_{\text{ref}} = \rho_e u_e C_{H_o}' H_e \tag{10}$$

where $\rho_e u_e C_{H_o}'$ is the nonablating heat-transfer coefficient evaluated at the ablation temperature.

The reason for normalizing by q_{ref} in the Eq. (9) correlation is that q_w can approach zero under conditions of very large blowing (in which case the transfer-coefficient reduces to zero) or when surface temperatures are elevated (in which case the driving potential can be zero). The use of q_{ref} as a normalizing parameter tends to de-emphasize the importance of solutions where these events occur so that the correlation will be the most accurate when heat-transfer rates are high. Certainly, it is not necessary to maintain the same percentage accuracy in q_w (or in $\rho_e u_e C_H'$ for that matter) as $q_w \to 0$.

Transfer-Coefficient Correlations

The BLIMP program described previously was employed to obtain a matrix of equal diffusion solutions for the stagnation-point boundary layer over various ablating nose cone materials. These boundary-layer solution data were then correlated in terms of heat- and mass-transfer coefficients. A primary objective of the study was to develop correlations which are independent of materials and flight conditions, and which apply for transient as well as steady-state conditions. Nonsimilar BLIMP solutions were also generated for laminar and turbulent boundary layers about sphere cones. These data are also presented in this section and compared to predictions based on direct application of the stagnation-point correlations.

Stagnation-point boundary-layer solutions were generated for graphite, carbon phenolic, and nylon phenolic for flight conditions ranging from total enthalpies of 500–13,000 Btu/lb and stagnation pressures of 0.01–150 atm. Three basic classes of solutions were obtained. 1) Steady-state ablation. The surface boundary condition here consists of surface equilibrium, a steady-state energy balance, and elemental mass balances; thus, surface ablation rates and surface temperatures as well as convective heating rates are calculated during the course of the solutions. 2) Virgin material ablation at nonsteady-state surface temperatures. These solutions are identical to 1 except that the surface energy balance is replaced by the assignment of surface temperature. 3) Simulated transient ablation. These solutions are identical to 2 except that pyrolysis gas injection rates are also assigned. Thus char recession rates and convective heating rates necessary to maintain surface equilibrium and to satisfy wall elemental mass balances are calculated as part of the solution. An extensive matrix of flight conditions was considered for each of the three materials for the first class of solutions; partial matrices were considered for the other two types of solutions. The results of these solutions are tabulated in Ref. 7.

Stagnation-Point Mass-Transfer Coefficient Correlations

An approach often used in the past[13] has been to correlate a heat-transfer coefficient in terms of a nonablating heat-transfer

‡ Rosner[8] employs a recovery factor for edge chemical enthalpy $r_{D,i}$ in lieu of C_{M_i}/C_H in Eq. (4) and suggests that $r_{D,i} \approx Le_{f,i}^n$ with $n = \frac{2}{3}$ for general application. Here $Le_{f,i}$ are Lewis numbers based on diffusion coefficients for species i diffusing through the mixture. Spalding[9] expresses his results directly in terms of $Le_{f,i}^{2/3}$.

§ Alternatively, consistent with whichever definition of $\rho_e u_e C_H'$ is used, the H_e in Eq. (8) can be replaced by the recovery enthalpy H_r.

coefficient and a blowing correction, and to obtain the mass-transfer coefficient from the heat-transfer coefficient through use of the Chilton-Colburn analogy [Eq. (6)]. Alternatively, one could employ a blowing correction to obtain the mass-transfer coefficient and obtain the heat-transfer coefficient through either a Chilton-Colburn type analogy or a second blowing correction. Investigation of the heat- and mass-transfer coefficients generated in the present study indicates clearly that the mass-transfer coefficient is much better behaved than the heat-transfer coefficient. Therefore, the latter approach has been adopted.

Blowing corrections are often expressed logarithmically in the form

$$C_M/C_{H_o}' = (1/2\lambda_m B')\ln(1 + 2\lambda_m B') = \phi_m/(e^{\phi_m} - 1) \quad (11)$$

where B' is the thermodynamic blowing parameter, $B' = \dot{m}_w/\rho_e u_e C_M$, λ_m is a correlation parameter, $\dot{m}_w$ is the net mass flux of vapor into the boundary layer ($\dot{m}_g + \dot{m}_c$), ϕ_m is defined by $\phi_m \equiv 2\lambda_m B_o'$ and $B_o' \equiv \dot{m}_w/\rho_e u_e C_{H_o}'$.

Each stagnation-point boundary-layer solution provides a value of λ_m for perfect correlation. A satisfactory correlation of the λ_m values was obtained[7] by permitting λ_m to be a function of B_o' and $\mathcal{M}_w/\mathcal{M}_e$ where $\mathcal{M}_w$ is the molecular weight of the gas mixture at the wall and $\mathcal{M}_e$ is the molecular weight of the boundary-layer edge gas

$$\lambda_m = (1.012 + 0.018B_o' + 0.0814B_o'^2)(1.0 - F_1)$$
$$F_1 = (0.238 + 0.038B_o')\left(\frac{F_2 - 0.95}{0.60}\right)^{0.71} \quad (12)$$
$$F_2 = \begin{cases} 0.95 & \mathcal{M}_w/\mathcal{M}_e \le 0.95 \\ \mathcal{M}_w/\mathcal{M}_e & 0.95 < \mathcal{M}_w/\mathcal{M}_e < 1.55 \\ 1.55 & \mathcal{M}_w/\mathcal{M}_e \ge 1.55 \end{cases}$$

The resulting correlation equation for C_M/C_{H_o}' [i.e., Eq. (11) and Eq. (12)] is presented in Fig. 1. The C_M/C_{H_o}' calculated from the correlation equation are compared in Fig. 2 to the C_M/C_{H_o}' obtained from the BLIMP solution data. It can be seen that the correlation equation typically predicts the data within $\pm 2\%$. The percentage errors in $\rho_e u_e C_M$ become larger as C_M/C_{H_o}' approaches zero, but this is not serious since $\rho_e u_e C_M$ itself is becoming small relative to $\rho_e u_e C_{H_o}'$. It can be seen from Fig. 2 that some improvement in the correlation could be obtained if the materials were considered separately. However, the general correlation equation is sufficiently accurate that further effort here is probably not warranted.

Stagnation-Point Heat-Transfer Correlations

As mentioned previously, there are a number of ways for representing the surface convective heat flux q_w; these include blowing corrections for $\rho_e u_e C_H$ or $\rho_e u_e C_H'$, Eq. (5) or Eq. (7), the Chilton-Colburn analogy and variations thereof, Eq. (6), and the $\psi - \Delta H_c$ approach, Eq. (9). All of these methods have been investigated and the results are described in this section.

The first approach considered was the straightforward use of a blowing correction for $\rho_e u_e C_H$. The $\rho_e u_e C_H$ were calculated

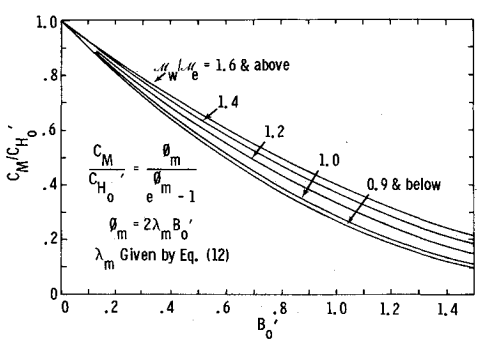

Fig. 1 Mass-transfer blowing-correction correlation.

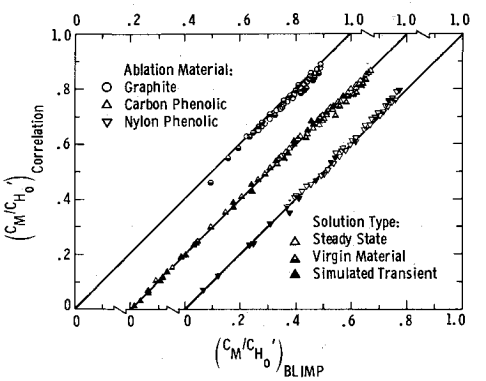

Fig. 2 Comparison of mass-transfer correlation with boundary-layer solution data.

from the BLIMP solutions using Eq. (5). The BLIMP solutions provide the $\rho_e u_e C_M$ as well as the q_w and the quantities which appear in the enthalpy potentials. The $\rho_e u_e C_H$ are then divided by $\rho_e u_e C_{H_o}'$ for the same flight condition and wall temperature. The resulting blowing correction did not correlate well.[7]

The Chilton-Colburn analogy as applied to $\rho_e u_e C_H$ and with an exponent n of $\frac{2}{3}$ [see Eq. (6)] is investigated in Fig. 3. The Lewis number employed in this correlation Le_w is based on the wall value of the effective diffusion coefficient employed in the BLIMP program equal-diffusion option.¶ The graphite solutions are seen to be represented quite well by the correlation, C_M/C_H differing from $Le_w^{2/3}$ by no more than 4% and being represented by a single correlation line within $\pm 1\%$. On the other hand, the carbon phenolic and nylon phenolic values of C_M/C_H differ substantially from $Le_w^{2/3}$. While curves are shown in Fig. 3 which represent virgin material ablation quite accurately, results for carbon phenolic for assigned B_g' [usually $B_g'/B_c' \gg (B_g'/B_c')_{ss}$] are seen to correlate better with the nylon phenolic results than with the carbon phenolic results. This is not too surprising since the pyrolysis gas compositions of the two materials are nearly the same. This would suggest that a single correlation curve applicable to all materials and conditions could possibly be obtained based on a parameter representative of the nature of the injected gas such as the percent of hydrogen. This was not attempted. Some effort was made to obtain correlations for the exponent n in Eq. (6) but these were not satisfactory.

A blowing correction for C_H'/C_{H_o}' is presented in Fig. 4. The solution data are presented separately for the three materials considered. A single curve is seen to represent the graphite data quite well. This curve was selected to fit not only the present data but the high enthalpy (and thus high blowing rate) graphite boundary-layer solution data of Ref. 14. The correlation of these two data sets is presented in Fig 5. This same

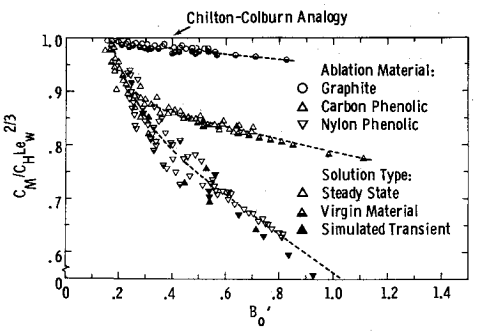

Fig. 3 Deviation of boundary-layer solution data from chilton-colburn analogy $C_M/C_H Le_w^{2/3} = 1.0$.

¶ The Le_w for steady-state ablation are nominally 0.98 for graphite, 0.85 for carbon phenolic, and 0.65 for nylon phenolic.

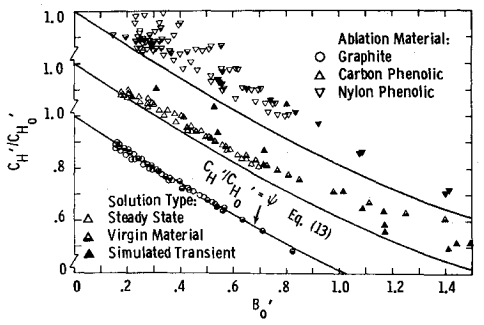

Fig. 4 Heat-transfer blowing-correlation C_H'/C_{H_0}'.

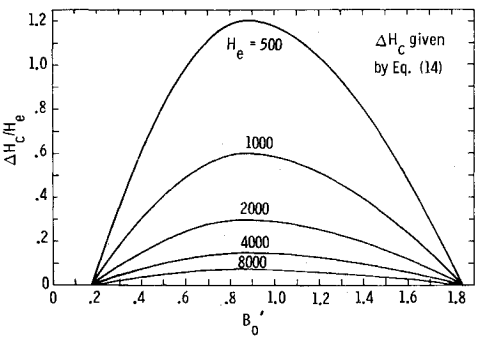

Fig. 6 Variation of $\Delta H_c/H_e$ with blowing rate and total enthalpy.

curve is also compared to the carbon phenolic and nylon phenolic data in Fig. 4 with the result that the solution data tend to be underpredicted by the correlation, especially in the case of nylon phenolic. Although it is not identified in Fig. 4, this deviation is strongly dependent upon the edge total enthalpy H_e as well as the blowing rate B_o'.

This observation led to the development of the $\psi - \Delta H_c$ correlation of Eq. (9). In particular, it is seen in Figs. 4 and 5 that graphite is represented well by the correlation

$$\psi = 1.0 - 0.6563B_o' + 0.01794B_o'^2 + 0.06365B_o'^3 - 0.01125B_o'^4 \tag{13}$$

with $\Delta H_c = 0$.** The carbon phenolic and nylon phenolic solutions were found[7] to correlate well with the same expression for ψ if ΔH_c is defined as

$$\Delta H_c = \begin{cases} 0 & B_o' \leq 0.17 \\ -600 + 1578(B_o' - 0.87)^2 + 503(B_o' - 0.87)^3 & 0.17 < B_o' \leq 0.87 \\ -600 + 805(B_o' - 0.87)^2 - 183(B_o' - 0.87)^3 & 0.87 < B_o' < 1.85 \\ 0 & B_o' \geq 1.85 \end{cases} \tag{14}$$

The ΔH_c is presented in Fig. 6 normalized by H_e since it is this term that is added to $\psi(H_e - h_w)/H_e$ in Eq. (9). The ΔH_c term, while typically small, can assume dominant importance for low values of H_e when $(H_e - h_w)/H_e$ is small [see Eq. (9)]. This trend in behavior is expected since the energy associated with reactions involving ablation products is relatively insensitive to H_e while the over-all convective heating typically increases with H_e.

The accuracy of this correlation is demonstrated in Fig. 7 where q_w/q_{ref} as computed from the correlation equations (9, 13, and 14), are shown vs q_w/q_{ref} as obtained from the BLIMP solutions. It can be seen that the errors are usually within 2–3% and seldom exceed 5%. This should be contrasted with heat-transfer coefficient correlations for which errors are unbounded at low H_e.[7]

In conclusion, a heat-transfer correlation has been developed which provides acceptably small errors in q_w relative to an appropriate reference condition. This correlation applies to all three materials considered, but this is done somewhat artificially since one of the parameters, ΔH_c, is set to zero for graphite. It is felt that a ΔH_c correlation could be devised (e.g., including a parameter such as percent hydrogen in the injected gas) which would treat all materials in a continuous manner. However, this extra degree of sophistication was not felt to be warranted.

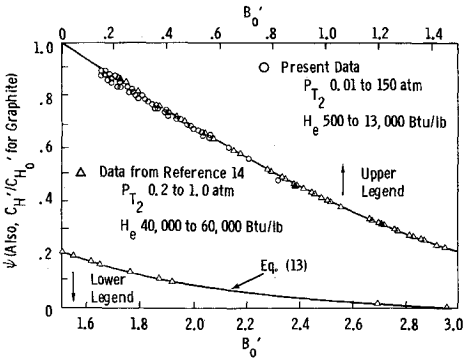

Fig. 5 Correlation of parameter ψ with graphite boundary-layer solution data.

**The parameter ψ is identical to C_H'/C_{H_o}' for $\Delta H_c = 0$.

Stagnation-Point Transient Flight Predictions

The ultimate test of transfer-coefficient correlations is to examine their accuracy when used in actual transient ablation predictions. Such a test was accomplished by performing several stagnation-point solutions for various materials and trajectories.[7] Results for carbon phenolic exposed to a relatively severe trajectory are presented here. The stagnation enthalpy H_e and total pressure behind the bow shock P_{T_2} considered in this calculation are presented in Fig. 8.

The transient ablation solution was generated with the CMA program[13] modified to accommodate the transfer-coefficient correlations recommended above, [Eqs. (11) and (12) for C_M/C_{H_o}' and Eqs. (9, 14, and 15) for q_w/q_{ref}]. The BLIMP program was then employed to obtain spot-check comparisons of transfer-coefficients and ablation rates for assigned values of pyrolysis gas rates and surface temperatures.

The CMA program treats one-dimensional transient conduction into a charring or noncharring material. It employs a surface thermochemical ablation model which is identical to that used in the BLIMP program except that the CMA program

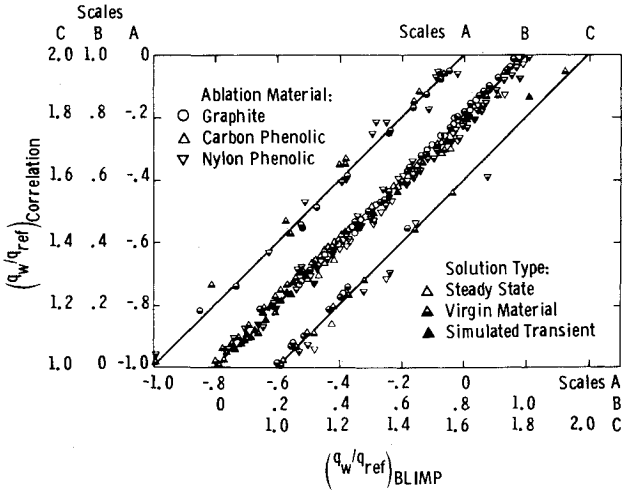

Fig. 7 Comparison of heat-transfer correlation q_w/q_{ref} with boundary-layer solution data.

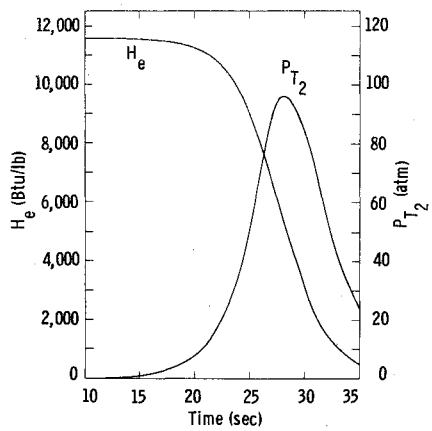

Fig. 8 Stagnation enthalpy and pressure for ballistic entry trajectory.

computes the surface heat and mass fluxes in terms of transfer coefficients, whereas BLIMP computes these quantities directly from boundary-layer profiles. It has been demonstrated[5] that when the transfer coefficients used in the CMA program represent the surface heat and mass fluxes exactly, the CMA and BLIMP programs yield identical results except for possible numerical errors.

The transient CMA flight predictions for the surface temperature T_w, convective heat-transfer rate q_w, surface ablation rate $\dot{m}_c$, and pyrolysis gas rate $\dot{m}_g$ are presented in Fig. 9. The spot-check BLIMP results for q_w and $\dot{m}_c$ are also shown (recall that T_w and $\dot{m}_g$ were used as input to the BLIMP program). The agreement between the BLIMP and CMA solutions for the two parameters is within 3% and 1%, respectively, consistent with the accuracy of the basic correlations.

Application of Stagnation-Point Correlations to Positions around the Body

The BLIMP program was employed to obtain laminar and turbulent boundary-layer solutions around graphite and carbon phenolic sphere cones for several representative flight conditions.[7] These solutions were generated considering surface equilibrium while satisfying a steady-state surface energy balance. Nonsimilar boundary-layer solutions considering entropy layer effects were considered in most cases. While a number of solutions are reported in Ref. 7, only two cases are presented here in detail: laminar and turbulent nonsimilar flow over a carbon phenolic sphere cone ($R_N = 0.4125$ in., $\theta_c = 9°$) including entropy layer effects at trajectory time 23.5 from Fig. 8 ($H_c = 10{,}147$ Btu/lb, $P_{T_2} = 33.18$ atm). Compared to conventional transition criteria such as that of Ref. 15, one would suspect turbulent flow over at least the majority of the heatshield at this flight condition. Thus, the laminar solution, while representative of the type of behavior that would be expected if laminar flow persisted, is not likely to occur.

The $\rho_e u_e C_M$ resulting from the BLIMP solutions are compared to values computed from the stagnation-point correlation in Fig. 10a. This is accomplished by considering the local values of the molecular weight ratio $\mathcal{M}_w/\mathcal{M}_e$, ablation rate $\dot{m}_w$, and nonablating laminar or turbulent heat-transfer coefficient $\rho_e u_e C_{H_o}'$, respectively. As suggested previously, the $\rho_e u_e C_{H_o}'$ can be defined in terms of edge total enthalpy or recovery enthalpy. Both approaches are examined in Fig. 10a.

In the laminar case, the only events which would not be expected to correlate well with the stagnation-point correlations are nonsimilar events associated with mass transfer since in applying the stagnation-point correlations to positions around the body the local transfer coefficients are normalized by the local nonsimilar nonablating heat-transfer coefficients. The laminar $\rho_e u_e C_M$ correlation is excellent in the blunt-body region ($S/R_N < 1.0$). The use of H_e and H_r is immaterial here since they are virtually the same. In the vicinity of the sphere-cone tangent point, the laminar BLIMP solution is seen to dip well below the results predicted by the stagnation-point correlation equations. This is the result of decreased ablation rates which arise because carbon vapor generated in the stagnation region is swept downstream. The effect was discussed previously for graphite.[16] This dip persists to rather large S/R_N (the order of 10). At very large S/R_N, excellent correlation is again achieved by the use of H_r in the $\rho_e u_e C_{H_o}'$ definition. The correlation based on H_e is about 20% low. The dip in laminar $\rho_e u_e C_M$ due to nonsimilar effects is much less pronounced for flight conditions sufficiently less severe that laminar flow would be expected.[7] It can be seen in Fig. 10a that the effect is much less severe for turbulent flow. Also, it can be seen that the stagnation-point correlation underpredicts the turbulent $\rho_e u_e C_M$ and that again H_r is better than H_e.

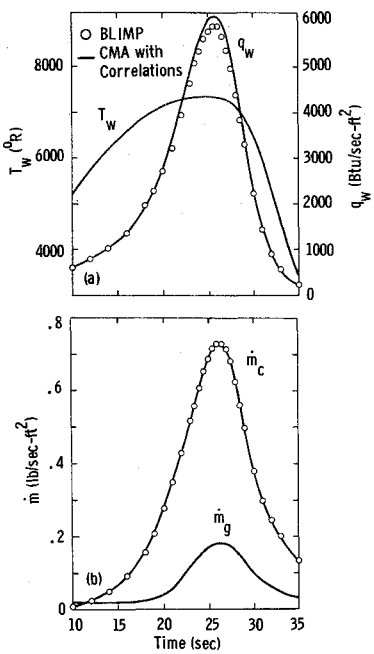

Fig. 9 Transient conduction solution for carbon phenolic stagnation point.

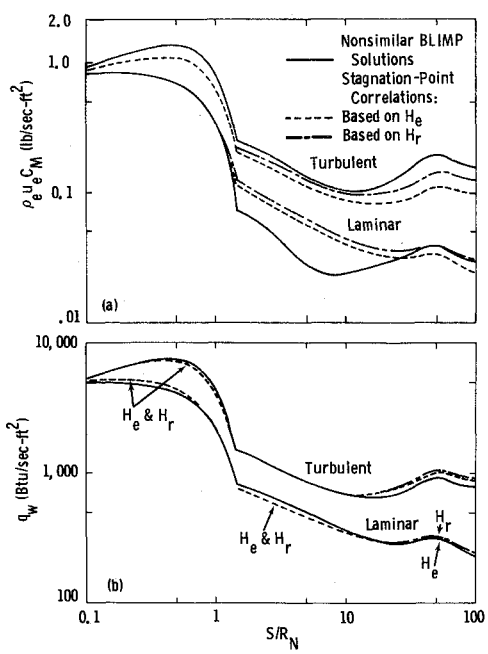

Fig. 10 Comparison of correlations with nonsimilar boundary-layer solutions.

Laminar and turbulent heat-transfer rates are presented in Fig. 10b. Laminar nonsimilar heat-transfer rates are predicted quite accurately with the stagnation-point correlation in contrast to the large dip in $\rho_e u_e C_M$. The choice between H_e and H_r is seen to be inconsequential. The influence of H_e vs H_r is largely cancelled out by the use of a consistent normalizing parameter q_{ref}. Turbulent heating rates are also predicted quite well with the stagnation-point correlation except for very large values of S/R_N where the correlations actually overpredict the heating rates by 10%. Similar trends were seen for graphite and other carbon phenolic solutions reported in Ref. 7.

Direct Transfer-Coefficient Approach

A transfer-coefficient approach was also developed for obtaining coupled solutions between the boundary-layer and heatshield transient response without intermediary blowing-correction correlations. The method employed is an iterative one which alternates between detailed boundary-layer and transient heat-conduction solutions until substantial agreement occurs.

The direct transfer-coefficient approach is shown schematically in Fig. 11 for the simple case of a homogeneous material. The iteration starts with an assumed T_w distribution input to the BLIMP program for each trajectory condition of interest. BLIMP uses this input to achieve assigned temperature surface equilibrium boundary-layer solutions. These solutions provide $\tilde{j}_{k_w}$, q_w, and the necessary potential terms to obtain $\rho_e u_e C_M$ and $\rho_e u_e C_H'$ from Eqs. (3) and (7), respectively. These coefficients together with surface equilibrium elemental mass balance tables obtained from the ACE program[17] are used to achieve an indepth transient heat-conduction solution with the CMA[13] program. The T_w computed by CMA is then compared with the original assumed T_w input to BLIMP. If they agree (i.e., within a small error), a converged solution has been obtained. If they do not agree, the T_w computed by CMA is cycled back into BLIMP and the iteration continues until convergence is achieved.†† When convergence is obtained all other surface properties such as q_w, $\dot{m}_c$, h_w, etc., are identical in both solutions because, as discussed previously, both satisfy the same surface boundary conditions. Thus, a fully-coupled solution of the ablating-surface boundary-layer problem is obtained.

Although this approach is iterative, it tends to converge rapidly because the transfer coefficients employed in the method are not strongly dependent upon surface temperature effects. For a typical graphite heat-shield under ballistic re-entry conditions, the difference in T_w was found to be less than 1% after two iterations.

Application of Direct Approach to Positions around the Body

At the stagnation point, the boundary layer is similar and the coupled solution can be obtained independent of solutions at any other body station (neglecting any shape change and multidimensional heat-conduction effects). However, at positions around the body it is necessary to consider a sequence of upstream body stations in order to achieve full coupling at the station of interest, except when local similarity approximations are adequate. The $\rho_e u_e C_{H_o}'$, $\rho_e u_e C_H'$, and $\rho_e u_e C_M$ for laminar and turbulent nonsimilar and locally similar boundary-layer solutions were compared for a typical steady-state graphite ablation problem. It was found that locally-similar transfer coefficients are within a few percent of those considering nonsimilar flow for $S/R_N < 1$ and $S/R_N > 20$. At intermediate S/R_N, substantial deviation can occur (especially in $\rho_e u_e C_M$[16]). Solutions presented in the following section were all performed at values of $S/R_N > 20$ where local similarity approximations are adequate.

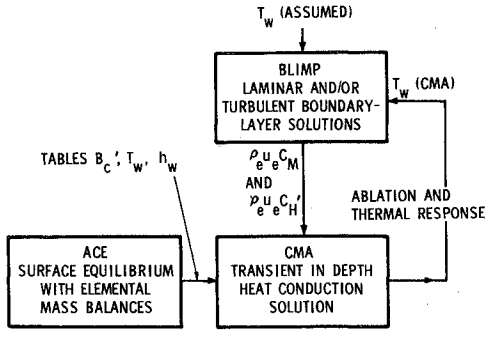

Fig. 11 Direct transfer-coefficient approach.

†† For charring ablators, $\dot{m}_g$ and T_w are iterated. ACE tables would contain B_g' as well as B_c'.

Comparison of Direct and Correlation Approaches with Flight Thermal Data

Sandia Laboratories, Albuquerque, has successfully flight tested several carbon/carbon composite heatshields under ballistic re-entry conditions. Carbon/carbon composites consist of a fibrous carbon substrate in a carbonaceous matrix. The carbon matrix is produced by the chemical vapor deposition (CVD) of carbon from a hydrocarbon gas. The fabrication processes associated with two representative carbon composites, CVD/felt and CVD/filament-wound, are described in Refs. 18 and 19, respectively.

The flight test configuration consisted of a sphere cone body ($R_N = 0.4125$ in., $\theta_c = 9°$) with an ATJ-S graphite nosetip and a carbon/carbon composite aftshield. While excellent temperature data were obtained on all flights, only two sets of data are presented here; the others yield similar results. Normalized backface temperatures (T/T_{max}) obtained from three thermal sensors, equally positioned around the same vehicle circumference, are presented in Figs. 12a and b for flights A and B, respectively. Typically, the three sensors agreed with each other within 10% for each flight.

Also shown in Figs 12a and b are the normalized backface temperature predictions and normalized surface heat fluxes calculated with the direct transfer-coefficient approach described previously. Briefly, locally-similar chemically-reacting ablating BLIMP boundary-layer solutions were generated to supply the transfer coefficients used in CMA to calculate the transient heatshield ablative and thermal response. Surface temperatures were iterated until values computed by CMA agreed within 1%

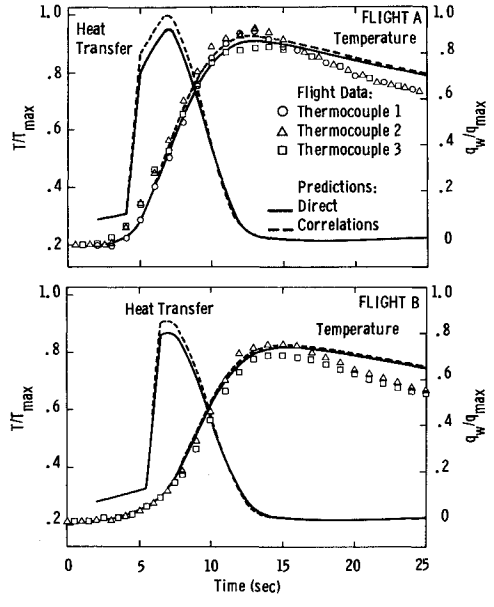

Fig. 12 Comparison of direct and correlation predictions with thermocouple response.

of those used in BLIMP. Figures 12a and b show that the final backface temperature predictions are within the scatter of the data during the heating portion of both flights. However, the calculations tend to overpredict the data by as much as 10% during the cooling portion. Similar trends were also obtained for the other body stations and flights. Possibly this is due to the surface equilibrium assumption employed in the calculations. The CVD process used in composite material fabrication tends to produce significant amounts of pyrolytic graphite[18] which can be kinetically controlled at these surface temperatures.[20] Calculations employing an approximate kinetically controlled ablation model[20] have been performed which give better agreement with the flight data; however, additional work must be done to validate the model.

Backface temperature predictions and surface heat fluxes were also calculated with the transfer-coefficient correlation approach. Briefly, these solutions were generated with the CMA program, modified to accommodate the transfer-coefficient correlations recommended for C_M/C_{H_o}' and q_w/q_{ref}. Locally-similar non-ablating BLIMP solutions provided the requisite $\rho_e u_e C_H'$. The correlation predictions are seen in Figs 12a and b to yield accuracies comparable with the direct transfer-coefficient approach and yield excellent agreement with the flight thermal data.

Summary of Results and Conclusions

Correlations of stagnation-point heat- and mass-transfer coefficients are developed which apply accurately over realistic ballistic entry conditions to graphite and to representative reinforced plastics. The matrix of solutions and the resulting correlations are sufficiently general that they would be expected to apply to other ablation materials and flight conditions as well as long as the principal surface material is graphitic or carbonaceous char.

In order to validate further the stagnation-point correlations, transient ablation and internal conduction solutions were generated and compared to equivalent boundary-layer solutions. Excellent agreement is obtained.

These same stagnation-point correlations are then applied to nonsimilar laminar and turbulent flows about sphere cones under typical ballistic entry conditions. They satisfactorily approximate heat transfer for turbulent as well as laminar flows to about 10%.

In the case of mass transfer, the correlations perform very well in the blunt-body region and well back on the cone ($S/R_N > 20$). For laminar flow, the nonsimilar $\rho_e u_e C_M$ can be substantially below the stagnation-point correlations. This discrepancy increases as the severity of the flight condition increases. However, conditions sufficiently severe to cause a large discrepancy may often be sufficiently severe to cause transition to turbulent flow for which the nonsimilar dip in $\rho_e u_e C_M$ is substantially smaller.

A procedure is also demonstrated for predicting heatshield ablation and thermal response with transfer coefficients given directly by boundary-layer solutions without intermediary transfer-coefficient correlations. Agreement between the direct approach, stagnation-point correlations, and heatshield flight data is seen to be excellent.

References

[1] Bartlett, E. P., Nicolet, W. E., Anderson, L. W., and Kendall, R. M., "Further Studies of the Coupled Chemically Reacting Boundary Layer and Charring Ablator," Aerotherm Rept. 68-38, Pt. I, Oct. 15, 1968, Aerotherm Corp., Mountain View, Calif.

[2] Kendall, R. M. and Bartlett, E. P., "Nonsimilar Solution of the Multicomponent Laminar Boundary Layer by an Integral-Matrix Method," *AIAA Journal*, Vol. 6, No. 6, June 1968, pp. 1089–1097.

[3] Anderson, L. W., Bartlett, E. P., and Kendall, R. M., "User's Manual Boundary Layer Integral Matrix Procedure (BLIMP)," Air Force Weapons Lab. Rept. AFWL-TR-69-114, March 1970, Vols. 1 and 2, Aerotherm Corp., Mountain View, Calif.

[4] Kendall, R. M., Anderson, L. W., and Aungier, R. H., "Nonsimilar Solution for Laminar and Turbulent Boundary-Layer Flows over Ablating Surfaces," *AIAA Journal*, Vol. 10, No. 9, Sept. 1972, pp. 1230–1236.

[5] Bartlett, E. P. and Grose, R. D., "An Evaluation of a Transfer Coefficient Approach for Unequal Diffusion Coefficients," Sandia Rept. SC-CR-69-3270, June 1969, Aerotherm Corp., Mountain View, Calif.

[6] Kendall, R. M., Rindal, R. A., and Bartlett, E. P., "A Multicomponent Boundary Layer Chemically Coupled to an Ablating Surface," *AIAA Journal*, Vol. 5, No. 6, June 1967, pp. 1063–1071.

[7] Bartlett, E. P. and Putz, K. E., "Heat- and Mass-Transfer Blowing-Correction Correlations for Charring Ablators, Pt. I, Equal Diffusion Coefficients," Sandia Rept. SC-RR-71-0260, Nov. 1971, Sandia Lab., Albuquerque, N. Mex.

[8] Rosner, D. E., "Convective Heat Transfer with Chemical Reaction," Aeronautical Research Lab. ARL 99, Aug. 1961, Aerochem Research Lab. Inc., Princeton, N. J.

[9] Spalding, D. B., *Convective Mass Transfer, An Introduction*, McGraw-Hill, New York, 1963.

[10] Fay, J. A. and Riddell, R. F., "Theory of Stagnation-Point Heat Transfer in Dissociated Air," *Journal of the Aeronautical Sciences*, Vol. 25, No. 2, Feb. 1958, pp. 73–85, 121.

[11] Lees, L., "Convective Heat Transfer with Mass Addition and Chemical Reactions," *Third AGARD Colloquium on Combustion and Propulsion*, Pergamon Press, New York, 1959.

[12] Mickley, H. S., Ross, R. C., Squyers, A. L., and Stewart, W. E., "Heat, Mass, and Momentum Transfer for Flow over a Flat Plate with Blowing or Suction," TN 3208, 1954, NACA.

[13] Moyer, C. B. and Rindal, R. A., "An Analysis of the Coupled Chemically Reacting Boundary Layer and Charring Ablator, Pt. II, Finite Difference Solution for the In-Depth Response of Charring Materials Considering Surface Chemical and Energy Balances," NASA CR-1061, June 1968, Aerotherm Corp., Mountain View, Calif.

[14] Bartlett, E. P., Nicolet, W. E., and Howe, J. T., "Heat-Shield Ablation at Superorbital Reentry Velocities," *Journal of Spacecraft and Rockets*, Vol. 8, No. 5, May 1971, pp. 456–463.

[15] Morkovin, M. V., "Critical Evaluation of Transition from Laminar to Turbulent Shear Layers with Emphasis on Hypersonically Traveling Bodies," Air Force Flight Dynamics Lab. Rept. AFFDL-TR-68-149, March 1969, RIAS, Martin Marietta Corp., Baltimore, Md.

[16] Bartlett, E. P., "Nonsimilar Behavior of Ablating Graphite Sphere Cones," *AIAA Journal*, Vol. 8, No. 5, May 1970, pp. 948–950.

[17] Powars, C. A. and Kendall, R. M., "User's Manual, Aerotherm Chemical Equilibrium (ACE) Computer Program," May 1969, Aerotherm Corp., Mountain View, Calif.

[18] Stroller, H. M. and Frye, E. R., "Processing of Carbon/Carbon Composites—An Overview," SC-DC-71 3653, April 1971, Sandia Labs., Albuquerque, N. Mex.

[19] Frye, E. R., "Carbon-Carbon Materials for Ablative Environments," SC-DC-70-5157, April 1971, Sandia Labs., Albuquerque, N. Mex.

[20] Maahs, H. C., "Oxidation of Carbon at High Temperatures: Reaction-Rate Control or Transport Control," TN D-6310, June 1971, NASA Langley Research Center, Hampton, Va.